2D13C-13C MAS NMR Correlation spectroscopy with mixing by true 1H spin diffusion reveals long-range intermolecular distance restraints in ultra high magnetic field

Boer, I. de; Bosman, L.; Raap, J.; Oschkinat, H.; Groot, H.J.M. de

Journal of Magnetic Resonance **157,** 286–291 (2002)
doi:10.1006/jmre.2002.2588

COMMUNICATION

2D ^{13}C–^{13}C MAS NMR Correlation Spectroscopy with Mixing by True ^{1}H Spin Diffusion Reveals Long-Range Intermolecular Distance Restraints in Ultra High Magnetic Field

Ido de Boer,* Leon Bosman,* Jan Raap,* Hartmut Oschkinat,† and Huub J. M. de Groot*,[1]

*Leiden Institute of Chemistry, Gorlaeus Laboratory, Einsteinweg 55, P.O. Box 9502, 2300 RA Leiden, the Netherlands; and †Forschungsinstitut für Molekulare Pharmakologie, Robert-Rössle Str. 10, D-13125, Berlin, Germany

Received November 26, 2001; revised June 17, 2002; published online August 28, 2002

An improved 2D ^{13}C–^{13}C CP^3 MAS NMR correlation experiment with mixing by true ^{1}H spin diffusion is presented. With CP^3, correlations can be detected over a much longer range than with direct ^{1}H–^{13}C or ^{13}C–^{13}C dipolar recoupling. The experiment employs a ^{1}H spin diffusion mixing period τ_m sandwiched between two cross-polarization periods. An optimized CP^3 sequence for measuring polarization transfer on a length scale between 0.3 and 1.0 nm using short mixing times of 0.1 ms < τ_m < 1 ms is presented. For such a short τ_m, cross talk from residual transverse magnetization of the donating nuclear species after a CP can be suppressed by extended phase cycling. The utility of the experiment for genuine structure determination is demonstrated using a self-aggregated Chl *a*/H_2O sample. The number of intramolecular cross-peaks increases for longer mixing times and this obscures the intermolecular transfer events. Hence, the experiment will be useful for short mixing times only. For a short $\tau_m = 0.1$ ms, intermolecular correlations are detected between the ends of phytyl tails and ring carbons of neighboring Chl *a* molecules in the aggregate. In this way the model for the structure, with stacks of Chl *a* that are arranged back to back with interdigitating phytyl chains stretched between two bilayers, is validated.

Key Words: **MAS NMR; spin diffusion; intermolecular correlations; distance restraints; phase cycling; correlation spectroscopy.**

INTRODUCTION

For systems of biological interest, supramolecular systems, and self-assembled nanodevices, solid state NMR in conjunction with uniform isotope enrichment offers an attractive route to resolve and refine microstructure (*1*). First, a series of homonuclear and heteronuclear correlation experiments are performed to assign the NMR response to the chemical structure. During this stage, much can be learned about the electronic properties of the system and nonbonding interactions, for example by comparing the solid state shifts with solution NMR data. In a next step, hydrogen bonding interactions within the system can be investigated (*2–4*). Finally, invaluable information about the structural arrangement can be obtained from measurement of intermolecular correlations, which involves transfer over relatively large distances of ~0.5 nm. While many strategies exist nowadays for assignment studies and characterization of hydrogen bonds, intermolecular transfer in uniformly labeled systems is not yet straightforward (*5–9*). In particular, detection of intermolecular ^{13}C–^{13}C correlations with dipolar recoupling techniques or proton-driven spin diffusion is very difficult, due to rapid relayed spin diffusion along the multispin ^{13}C-labeled molecular network in uniformly enriched systems (*10*).

At an early stage, the use of MAS NMR correlation spectroscopy to resolve the structure of a uniformly enriched solid has been demonstrated for self-aggregated chlorophyll *a*/H_2O (*1, 11*). Chl *a* constitutes the green pigment in the photosynthetic apparatus of plants as well as algae and cyanobacteria. It is responsible for the absorption of light and essential for the subsequent conversion of the excitation energy into chemical energy. The chemical structure of Chl *a* is depicted in Fig. 1A. When exposed to H_2O it forms an aggregate. Such aggregates represent a paradigm for chlorophyll stacking in the chlorosome light-harvesting antennae found in some green photosynthetic bacteria (*12, 13*). Thus, chlorophyll aggregates can form protein-free light-harvesting antennae, which is of potential interest for artificial photosynthesis.

To resolve a model for the 3D stacking in self-aggregated, uniformly enriched chlorophyll *a*/H_2O with MAS NMR, ^{13}C and ^{1}H chemical shifts were assigned by means of ^{13}C–^{13}C homonuclear and ^{1}H–^{13}C heteronuclear dipolar correlation spectroscopy (*1, 11*). Shift constraints and intermolecular correlations obtained from a long-range ^{1}H–^{13}C experiment were used to construct a space-filling model (*11*). In this paper ^{1}H spin diffusion techniques are used to detect intermolecular

[1] To whom correspondence should be addressed. Fax: +31 (0)71 527 4603. E-mail: groot_h@chem.leidenuniv.nl.

1090-7807/02 $35.00

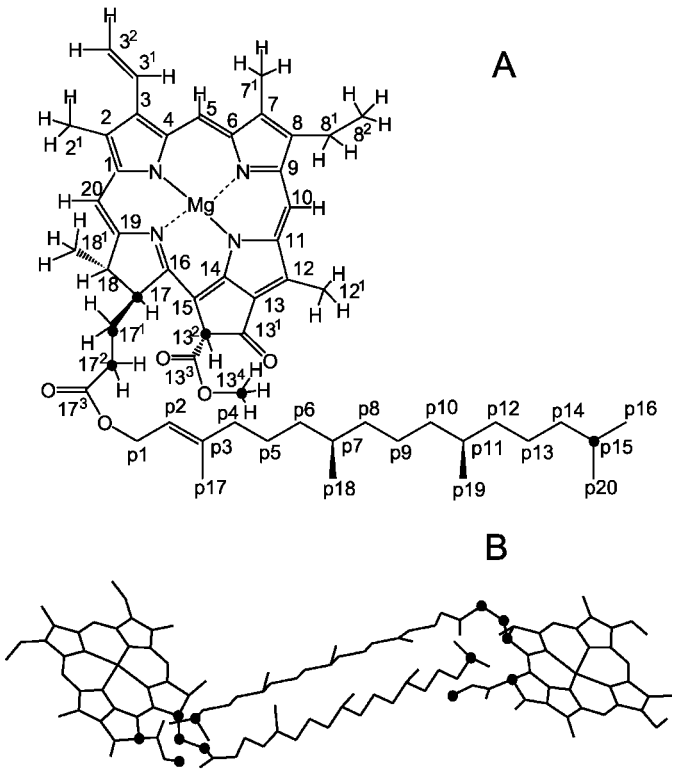

FIG. 1. Chemical structure of Chl *a* with the IUPAC numbering for the ring (A). For the phytyl tail the prefix P is used. The ^{1}H atoms are shown explicitly for the ring only. The proposed structural arrangement of the two Chl *a* molecules in the unit cell of self-aggregated Chl *a*/H_2O is depicted below (B). The hydrogens are left out for clarity. Solid circles indicate the carbons involved in the intermolecular correlations.

^{13}C–^{13}C correlations (*14, 15*). A modified CP^3 experiment is presented, optimized for short ^{1}H mixing times 0.1 ms $< \tau_m <$ 1 ms. Correlations spanning distances between 0.1 and 1.0 nm are easily generated. Intermolecular cross-peaks are observed in the self-aggregated chlorophyll *a*/H_2O that lead to a validation and refinement of the existing model for the stacking (*1, 11*).

RESULTS AND DISCUSSION

Since protons constitute a dense network of strongly coupled spins, ^{1}H spin diffusion is an attractive way to investigate structural properties on a nm length scale (*16*). The polarization exchange between ^{1}H spins is in principle a coherent process subject to relaxation (*17*). However, for many spins, with varying coupling strengths and sufficiently long transfer times, the spin dynamics can be described in terms of a classical diffusion model (*16*). For rigid organic materials, diffusivities of $\sim$0.8 nm^2/ms have been reported and ^{1}H spin diffusion allows the determination of the morphology of polymers over a very long range, up to ca. 200 nm (*16, 18*). This value for the diffusivity has also been used for experiments employing moderate MAS frequencies (*14–16, 19–21*). The favorable polarization transfer properties of ^{1}H can be combined with the superior spectral resolution of ^{13}C nuclei in a 2D ^{13}C–^{13}C MAS CP^3 correlation spectroscopy experiment (*14, 15*). In an early application of this method, the morphology and phase separation of ^{13}C-labeled semi-interpenetrating networks were investigated (*15, 20*). In the solid state NMR of complex solid-type biological assemblies, for example membrane proteins, the same principles could be applied to probe shorter range intra- and intermolecular distances for structure determination.

Figure 2 shows a CP^3 pulse scheme that is optimized for short mixing times, 0.1 ms $< \tau_m <$ 1 ms. During the preparation period ^{13}C transverse coherence is established with ramped cross polarization (*22*). The residual transverse ^{1}H magnetization is, ideally, rotated back to the *z*-axis. Next, free precession of ^{13}C is allowed during t_1, while TPPM irradiation on the ^{1}H channel is applied for heteronuclear decoupling (*23*). A second CP step transfers the t_1 modulated magnetization back to the protons. The ^{1}H magnetization is subsequently stored along the magnetic field B_0 by a 90° pulse. The distribution of ^{1}H *z* magnetization is allowed to equilibrate during a spin diffusion period τ_m. With another 90° pulse, the ^{1}H polarization is rotated back to the *XY* plane and a final CP is applied for high-resolution ^{13}C detection.

For short mixing times, $\tau_m \lesssim T_2$, the residual transverse magnetization from the donating nuclear species after the first two CP periods is a serious problem. Residual ^{1}H magnetization after the first CP interval interferes with the magnetization transfer during the second CP step. In addition, residual ^{13}C signal from the second CP interval mixes with the ^{13}C coherence created during the third CP period. These processes can give rise to strong artifacts in the 2D correlation spectrum.

The simplest way to deal with these cross-talk problems is a 90° pulse to rotate the remaining coherence after the first and second CP period along the *z*-axis. In practice, adequate

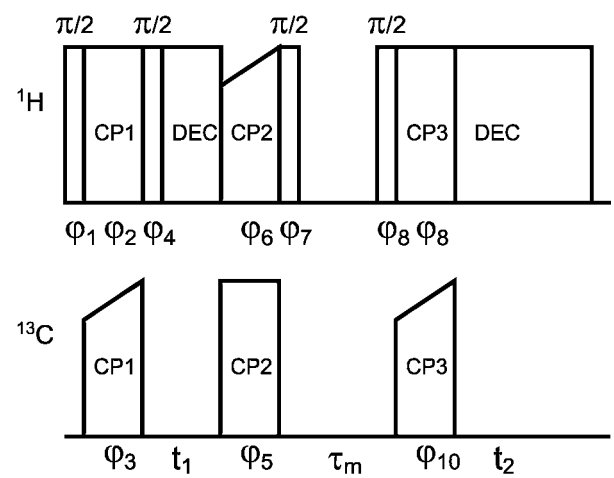

FIG. 2. Schematic representation of the extended CP^3 pulse sequence, suitable for the 2D ^{13}C–^{13}C MAS NMR correlation spectroscopy with a short ^{1}H spin–diffusion mixing period.

suppression of artifacts with a 90° pulse is difficult to achieve due to pulse imperfections, in particular for the ^{13}C. During rf irradiation, the effective field is tilted with respect to the z-axis by an angle θ such that

$$\tan(\theta) = \frac{B_1}{\Delta B_0}, \qquad [1]$$

where B_1 is the applied rf field strength and ΔB_0 the residual z-component of the magnetic field in the rotating frame. For off-resonance irradiation, θ deviates from 90° and the effective field points out of the XY plane. For a high-field spectrometer or moderate rf power and a broad chemical shift dispersion, this offset can become very significant for ^{13}C and the effect of the 90° pulse is spoiled. For example, for a spectrometer with a 750 MHz ^1H resonance frequency and using a moderate ~50 kHz rf power, ^{13}C spins shifted toward the extreme ends of a 300 ppm wide spectrum experience deviations (90°-θ) as high as ~30°. Due to a lower shift dispersion of ~14 ppm, this value is down to ~5° for ^1H spins under similar conditions.

After the first CP period, the residual ^1H transverse magnetization is thus only partially removed by a 90° pulse. By cycling the phase of the initial ^1H 90° pulse relative to the phase of the ^1H spin lock pulse of the second CP, contributions of the residual magnetization to the magnetization transfer during this CP step are cancelled (Table 1). Prior versions of the CP^3 experiment use a ^{13}C lock pulse after the first CP, which allows the residual ^1H signal to decay during a spin lock time $\tau > T_2$ (*14, 15*). In practice, this yields a considerable loss of the ^{13}C signal, in particular for materials with a long ^1H T_2. This disadvantage is avoided by the phase cycling of the initial ^1H 90° pulse.

The residual ^{13}C transverse magnetization after the second CP period vanishes only for a long $\tau_m \gg T_2$ (*15*). For shorter τ_m, the phase of the residual ^{13}C signal can be cycled relative to the phase of the ^{13}C signal detected during t_2 (*14*). In this way, the ^{13}C cross talk is eliminated. The pulse scheme of Fig. 2 with the cycling of Table 1 is straightforward to implement. Given that the signal to be cancelled has a considerable intensity, the phase alternation sequence of Table 1 needs to be rather extensive in order to compensate for any imperfections of the phase settings, precession during pulses, etc.

TABLE 1
Phase Alternation Scheme Corresponding with the Pulse Sequence of Fig. 2

φ_1	φ_2	φ_3[a]	φ_4	φ_5	φ_6	φ_7	φ_8	φ_9	φ_{10}	φ_{det}
+X	−Y	+Y	−X	+Y	−Y	+X	−X	+Y	+Y	−Y
+X	−Y	+Y	−X	+Y	+Y	+X	−X	+Y	+Y	+Y
−X	−Y	+Y	+X	+Y	−Y	+X	−X	+Y	−Y	−Y
−X	−Y	+Y	+X	+Y	+Y	+X	−X	+Y	−Y	+Y
+Y	+X	+Y	−Y	+Y	−Y	+X	−X	+Y	−X	+X
+Y	+X	+Y	−Y	+Y	+Y	+X	−X	+Y	−X	−X
−Y	+X	+Y	+Y	+Y	−Y	+X	−X	+Y	+X	+X
−Y	+X	+Y	+Y	+Y	+Y	+X	−X	+Y	+X	−X
−X	+Y	+Y	+X	+Y	−Y	+X	−X	+Y	−Y	+Y
−X	+Y	+Y	+X	+Y	+Y	+X	−X	+Y	−Y	−Y
+X	+Y	+Y	−X	+Y	−Y	+X	−X	+Y	+Y	+Y
+X	+Y	+Y	−X	+Y	+Y	+X	−X	+Y	+Y	−Y
−Y	−X	+Y	+Y	+Y	−Y	+X	−X	+Y	+X	−X
−Y	−X	+Y	+Y	+Y	+Y	+X	−X	+Y	+X	+X
+Y	−X	+Y	−Y	+Y	−Y	+X	−X	+Y	−X	−X
+Y	−X	+Y	−Y	+Y	+Y	+X	−X	+Y	−X	+X

[a] +TPPI for phase-sensitive detection in t_1.

For moderate MAS rates, ^1H spin diffusion processes can take place not only during the mixing time, but also during the CP intervals. In a static sample, the spin diffusion rate during a spin lock is effectively scaled by a factor of $\frac{1}{2}$ (*16*). Therefore, it is expected that the ^1H spin diffusion is slower during the CP periods. In addition, short CP times of 150 μs were used to prevent spin diffusion during CP from compromising the selectivity of the established correlations with respect to the distance. A 2D spectrum results, where only proton-bound carbons are visible (Fig. 3). Since these carbons usually cover a limited chemical shift range of only ~150 ppm, the spectral width can be reduced, yielding a shorter acquisition time of the 2D experiment, or a better resolution.

Using the sequence in Fig. 2, a series of datasets were collected from a sample of uniformly labeled self-aggregated Chl a/H_2O (Fig. 3). Each spectrum was obtained using a different mixing time in ~11 h with a spinning frequency $\omega_r/2\pi = 14.5$ kHz. An extensive discussion of the assignment of the ^{13}C NMR response can be found elsewhere (*11*). The CP transfer reaches its maximum in ~150 μs CP time. This was verified with a separate 1D ^1H–^{13}C CP MAS experiment (data not shown).

Several cross-peaks in Fig. 3 are indicated with arrows and labels. Dashed lines indicate the symmetry-related signals via the corresponding diagonal peaks. In order to quantify the transfer range of the correlation observed with these ^1H spin diffusion experiments, the distances between hydrogens directly bound to the carbons assigned to the cross-peaks are determined from the Chl a structure. For the shortest diffusion time $\tau_m = 100$ μs (Fig. 3A), most of the cross-peaks involve intramolecular correlations with a ^1H transfer range $\lesssim$4 Å. The 17 and the 13^4 ^{13}C resonate with 51.7 and 51.8 ppm chemical shift, respectively (*11*). Although the signals overlap in the 2D homonuclear correlation experiment, both labels are in the same region of the molecule and cross-peaks with other carbons can provide structural information. The same is true for the 17^1 and 17^2 signals, which coincide at 32.3 ppm. The 7^1 response is doubled at 8.9 and 11.5 ppm (Fig. 3), indicating two structurally distinct environments (*11*). The p15 ^{13}C signal is shifted to 28.4 ppm (*1, 11*) and is well resolved in the spectrum. In Fig. 3A, correlations of p15 with the 13^2 and with the overlapping 17^1,17^2, and 13^4,17 labels are clearly observed. The p15 carbons are located at the ends of the interdigitating phytyl tails, and these correlations are attributed to intermolecular polarization transfer during τ_m.

A CP^3 experiment with a longer $\tau_m = 200$ μs is shown in Fig. 3B. Some intramolecular correlations are detected that are not observed in the experiment with $\tau_m = 100$ μs (A). The

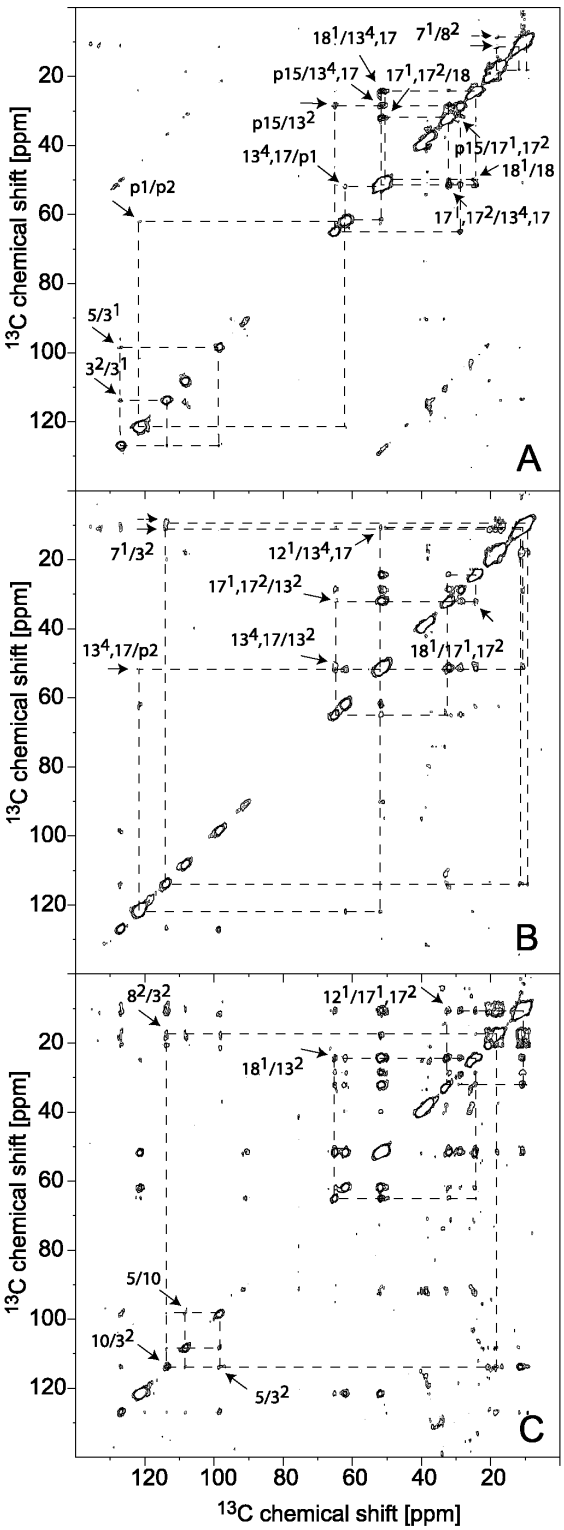

intramolecular ^{1}H transfer extends over ~7 Å. Finally, an experiment with a mixing time of 700 μs yields many cross-peaks (Fig. 3C). Several of the longer range correlations are depicted in Fig. 3C. Selective assignment between intra- and intermolecular correlations is virtually impossible for such a long diffusion time.

In a first order approximation, the protons form a chainlike or tubular arrangement at the exterior of the molecule. During spin diffusion in one dimension, the initial magnetization located at $r = 0$ spreads like a Gaussian distribution with a root-mean-square distance developing as

$$\sqrt{\langle r^2 \rangle} = \sqrt{2Dt}. \qquad [2]$$

Although a moderate spinning frequency of 14.5 kHz is used in these experiments, the characteristic diffusivity D of ~0.8 nm^2/ms commonly used in the literature is expected to be useful for a rough approximation. Equation [2] yields ~4 and ~6 Å for 100 and 200 μs mixing, respectively. Hence the actual intramolecular transfer range of ~4 Å for $\tau_m = 100$ μs and ~7 Å for $\tau_m = 200$ μs is in line with previous data for ^{1}H spin diffusion. For $\tau_m = 700$ μs, Eq. [2] predicts a spin diffusion range of ~11 Å. In that case the correlations can span the entire ring and an assignment to intra- or intermolecular transfer is difficult, in agreement with the data presented in Fig. 3C.

Based on aggregation shifts and long-range ^{1}H–^{13}C transfer, a model for the stacking of self-aggregated Chl *a*/H_2O was proposed, where parallel Chl *a* stacks are in a sheet arrangement, similar to that of ethyl chlorophyllide *a* (*1, 11*). In a first attempt to resolve the stacking in three dimensions, it was inferred from the data that the sheets form bilayers in a back-to-back arrangement with interdigitating chains, where several other models were rejected. The phytyl chains were assumed to be elongated, considering the linewidths of the phytyl carbons and the absence of conformational shifts.

The observed intermolecular correlations involving the p15 carbon provide a first direct experimental validation of the bilayer arrangement in the aggregate. The end of the phytyl tail of the Chl *a* molecule appears to be in close contact with the ring of a neighboring Chl *a*. From the spectra shown in Fig. 3, it can be concluded that the p15 proton is separated from hydrogens located near the basis of the phytyl tail by $\lesssim$4 Å. The only way to arrange the two Chl *a* bilayers to accommodate these distance restraints is shown schematically in Fig. 1B. The two Chl *a* moieties are from two adjacent bilayers and the carbons that are involved in the observable intermolecular correlations are depicted by solid circles in Fig. 1. According to our results,

FIG. 3. Contour plots of absorption mode 2D ^{13}C–^{13}C MAS NMR correlation spectra of aggregated Chl *a*/H_2O recorded with a spinning speed of 14.5 kHz in a field of 17.6 T and acquired with the sequence of Fig. 2. Arrows and labels are used to indicate cross-peaks, which are connected to the corresponding diagonal peaks and mirror peaks by dashed lines. Data were acquired with $\tau_m = 100$ μs (A), $\tau_m = 200$ μs (B), and $\tau_m = 700$ μs (C). For all experiments, a prescan delay of 1 s was used for a total of 192 scans for each of 200 t_1 points. A Lorentz–Gauss transformation with a line broadening of 60 Hz was applied to the datasets in the t_2 dimension prior to Fourier transformation. A sine–square apodization, phase shifted by $2\pi/3$, was used in the t_1 dimension.

the elongated phytyl tails are somewhat closer to the other ring than suggested in the earlier work (*1, 11, 24–26*).

Hence, the modified CP^3 experiment forms a useful complementary technique for the detection of intermolecular correlations over short distances >0.3 nm. It can be a valuable tool in a structure elucidation strategy. It is anticipated that the comparison of multiple datasets, recorded with varying mixing times, can lead to sets of distance constraints that provide information about, for example, the folding of a protein.

CONCLUSIONS

The 2D CP^3 ^{13}C–^{13}C MAS NMR correlation experiment with true ^1H spin diffusion previously implemented for long-range polarization transfer is successfully adapted for the detection of short-range intermolecular correlations in uniformly labeled systems of biological interest. Short mixing intervals 0.1 ms < $\tau_m < t$0.7 ms are used to detect intermolecular correlations spanning distances <1 nm. In this way, information about the structure of self-aggregated Chl a/H_2O is obtained. There is clear evidence for the proximity of the ends of the phytyl chains of Chl *a* rings of opposite stacks. With the phase cycling presented here, the CP^3 experiment offers an attractive method for the collection of intermolecular distance restraints and structural elucidation.

EXPERIMENTAL

The preparation of uniformly labeled self-aggregated Chl a/H_2O has been described before (*1*). The measurements were performed with a DSX-750 spectrometer and using a 4-mm triple resonance probe (Bruker, Germany), operating at a temperature of 298 K. The spinning frequency was kept constant within a few hertz. During the ^{13}C evolution intervals, heteronuclear TPPM decoupling (*23*) was applied with pulses of 7.3 μs and a phase modulation of 15°, using a rf nutation frequency of 66 kHz. Phase-sensitive detection in the t_1 dimension was simulated with a TPPI scheme (*27*).

ACKNOWLEDGMENTS

J. Hollander, F. Lefeber, and C. Erkelens are thanked for assistance during various stages of the experiments. H.J.M.d.G. is a recipient of a PIONIER award of the chemical sciences division of the Netherlands Organization for Scientific Research (NWO). The 750-MHz instrumentation was financed in part by Demonstration Project BIO4-CT97-2101 of the Commission of the European Communities.

REFERENCES

1. G. J. Boender, J. Raap, S. Prytulla, H. Oschkinat, and H. J. M. de Groot, MAS NMR structure refinement of uniformly C-13 enriched chlorophyll-a water aggregates with 2d dipolar correlation spectroscopy, *Chem. Phys. Lett.* **237,** 502–508 (1995).
2. B. J. van Rossum, C. P. de Groot, V. Ladizhansky, S. Vega, and H. J. M. de Groot, A method for measuring heteronuclear (H-1-C-13) distances in high speed MAS NMR, *J. Am. Chem. Soc.* **122,** 3465–3472 (2000).
3. X. Zhao, M. Eden, and M. H. Levitt, Recoupling of heteronuclear dipolar interactions in solid-state NMR using symmetry-based pulse sequences, *Chem. Phys. Lett.* **342,** 353–361 (2001).
4. S. P. Brown, X. X. Zhu, K. Saalwachter, and H. W. Spiess, An investigation of the hydrogen-bonding structure in bilirubin by H-1 double-quantum magic-angle spinning solid-state NMR spectroscopy, *J. Am. Chem. Soc.* **123,** 4275–4285 (2001).
5. S. Luca, D. V. Filippov, J. H. van Boom, H. Oschkinat, H. J. M. de Groot, and M. Baldus, Secondary chemical shifts in immobilized peptides and proteins: A qualitative basis for structure refinement under Magic Angle Spinning, *J. Biomol. NMR* **20,** 325–331 (2001).
6. E. Alberti, E. Humpfer, M. Spraul, S. M. Gilbert, A. S. Tatham, P. R. Shewry, and A. M. Gil, A high resolution H-1 magic angle spinning NMR study of high-M-r subunit of wheat glutenin, *Biopolymers* **58,** 33–45 (2001).
7. C. Ochsenfeld, S. P. Brown, I. Schnell, J. Gauss, and H. W. Spiess, Structure assignment in the solid state by the coupling of quantum chemical-calculations with NMR experiments: A columnar hexabenzocoronene derivative, *J. Am. Chem. Soc.* **123,** 2597–2606 (2001).
8. J. Pauli, M. Baldus, B. van Rossum, H. de Groot, and H. Oschkinat, Backbone and side-chain C-13 and N-15 signal assignments of the alpha-spectrin SH3 domain by magic angle spinning solid-state NMR at 17.6 tesla, *Chembiochem.* **2,** 272–281 (2001).
9. M. Hong, Determination of multiple phi-torsion angles in proteins by selective and extensive C-13 labeling and two-dimensional solid-state NMR, *J. Magn. Reson.* **139,** 389–401 (1999).
10. B. J. van Rossum, G. J. Boender, F. M. Mulder, J. Raap, T. S. Balaban, A. Holzwarth, K. Schaffner, S. Prytulla, H. Oschkinat, and H. J. M. de Groot, Multidimensional CP-MAS C-13 NMR of uniformly enriched chlorophyll, *Spectrochim. Acta Part A Mol. Biomol. Spectrosc.* **54,** 1167–1176 (1998).
11. B. J. van Rossum, E. A. M. Schulten, J. Raap, H. Oschkinat, and H. J. M. de Groot, A 3-D structural model of solid self-assembled chlorophyll a/H_2O from multispin labeling and MAS NMR 2-D dipolar correlation spectroscopy in high magnetic field, *J. Magn. Reson.* **155,** 1–14 (2002).
12. D. L. Worcester, T. J. Michalski, and J. J. Katz, Small-angle neutron scattering studies of chlorophyll micelles: Models for bacterial antenna chlorophyll, *Proc. Nat. Acad. Sci. U.S.A.* **83,** 3791–3795 (1986).
13. B. J. van Rossum, D. B. Steensgaard, F. M. Mulder, G. J. Boender, K. Schaffner, A. R. Holzwarth, and H. J. M. de Groot, A refined model of the chlorosomal antennae of the green bacterium Chlorobium tepidum from proton chemical shift constraints obtained with high-field 2-D and 3-D MAS NMR dipolar correlation spectroscopy, *Biochemistry* **40,** 1587–1595 (2001).
14. M. Wilhelm, H. Feng, U. Tracht, and H. W. Spiess, 2D CP/MAS C-13 isotropic chemical shift correlation established by H-1 spin diffusion, *J. Magn. Reson.* **134,** 255–260 (1998).
15. F. M. Mulder, W. Heinen, M. van Duin, J. Lugtenburg, and H. J. M. de Groot, Spin diffusion with C-13 selection and detection for the characterization of morphology in labeled polymer blends with MAS NMR, *J. Am. Chem. Soc.* **120,** 12,891–12,894 (1998).
16. K. Schmidt-Rohr and H. W. Spiess, "Multidimensional Solid-State NMR and Polymers," Academic Press, London (1994).
17. S. Zhang, B. H. Meier, and R. R. Ernst, Polarization echoes in NMR, *Phys. Rev. Lett.* **69,** 2149–2151 (1992).
18. J. Clauss, K. Schmidtrohr, and H. W. Spiess, Determination of domain sizes in heterogeneous polymers by solid-state NMR, *Acta Polym.* **44,** 1–17 (1993).
19. K. Landfester, C. Boeffel, M. Lambla, and H. W. Spiess, Characterization of interfaces in core–shell polymers by advanced solid-state NMR methods, *Macromolecules* **29,** 5972–5980 (1996).

20. F. M. Mulder, W. Heinen, M. van Duin, J. Lugtenburg, and H. J. M. de Groot, Cross-linking induced phase separation in SAN/SMA semi-interpenetrating polymer networks observed by solid state NMR and site specific isotope enrichment, *Macromolecules* **33,** 5544–5548 (2000).

21. K. K. Kumashiro, K. Schmidt-Rohr, O. J. Murphy, K. L. Ouellette, W. A. Cramer, and L. K. Thompson, A novel tool for probing membrane protein structure: Solid-state NMR with proton spin diffusion and X-nucleus detection, *J. Am. Chem. Soc.* **120,** 5043–5051 (1998).

22. G. Metz, X. L. Wu, and S. O. Smith, Ramped-amplitude cross-polarization in magic-angle-spinning NMR, *J. Magn. Reson. Ser. A* **110,** 219–227 (1994).

23. A. E. Bennett, C. M. Rienstra, M. Auger, K. V. Lakshmi, and R. G. Griffin, Heteronuclear decoupling in rotating solids, *J. Chem. Phys.* **103,** 6951–6958 (1995).

24. H. C. Chow, R. Serlin, and C. E. Strouse, The crystal and molecular structure and absolute configuration of ethyl chlorophyllide *a* dihydrate. A model for the different spectral forms of chlorophyll *a, J. Am. Chem. Soc.* **97,** 7230–7237 (1975).

25. G. Donnay, Crystal data on chlorophyll *a, Arch. Biochem. Biophys.* **80,** 80–85 (1959).

26. C. Kratky and J. D. Dunitz, Ordered aggregation states of chlorophyll *a* and some derivatives, *J. Mol. Biol.* **113,** 431–442 (1977).

27. D. Marion and K. Würthrich, Phase-sensitive COSY in proteins, *Biochem. Biophys. Res. Com.* **113,** 967 (1983).